Superthermal x-ray emission from CO_2-laser-produced plasmas

G. D. Enright, M. C. Richardson, and N. H. Burnett

Division of Physics, National Research Council of Canada, Ottawa, K1A 0R6 Canada
(Received 12 July 1978; accepted for publication 29 January 1979)

The high-energy continuum x-ray emission from plasma created by intense (10^{14} W cm^{-2}) nanosecond 10-μm laser pulses has been characterized. The temperature of the superthermal electron component deduced from this emission was found to be strongly dependent on focus position, while displaying a weaker dependence on irradiation angle, beam polarization, and target composition. The variation of the hot-electron temperature as a function of $I\lambda^2$ has been examined in detail in a range of $I\lambda^2$ from 10^{15} to 2×10^{16} Wμm^2 cm^{-2} for various target materials and has been found to be in qualitative agreement with the predictions of current theories of hot-electron production based on resonance absorption.

PACS numbers: 52.50.Jm, 52.70. – m

I. INTRODUCTION

Characterization of the x-ray continuum emission from laser-produced plasmas is a proven approach to the estimation of plasma temperatures and an important indicator of energy absorption and transport processes.[1–5] In recent times, examination of the x-ray continuum from plasmas produced by intense ($>10^{14}$ W cm^{-2} at 1.06 μm) nanosecond laser pulses has identified hard x-ray emission uncharacteristic of a purely thermal electron-energy distribution.[6–9] This has generally been interpreted as being due to the generation of superthermal electrons during the laser-light absorption process. Since these high-energy electrons play a critical role in laser-fusion schemes, it has become of considerable importance to determine their characteristics in terms of laser and focusing conditions, target configuration, and in particular their dependence on laser wavelength and intensity. The dependence on laser intensity is not only of concern in the design of laser-fusion targets, but also can be considered as an important signature of possible nonlinear processes occurring during the laser-plasma interaction.[10–17] While early calculations estimated the hot-electron temperature (T_H)[10] to scale with $I\lambda^2$ (the parameter $I\lambda^2$ is directly proportional to the oscillatory energy of an electron in the incident-radiation field) where I is the laser intensity and λ is its wavelength, other dependences have also been predicted. Theories based on flux limitation with stochastically heated electrons at the critical surface predict[11,13] $T_H \sim (I\lambda^2)^{2/3}$, whereas resonance absorption has been shown to indicate a dependence on either $(I\lambda^2)^{1/2}$ [14,15] or $(I\lambda^2)^{1/3}$.[16]

Experimentally, insofar as investigations with intense subnanosecond Nd : glass laser pulses ($\lambda = 1.06\,\mu$m) are concerned, reasonably consistent x-ray measurements of the variation of T_H with laser intensity have recently been reported by a number of laboratories.[9,18–20] Those are all compatible with resonance absorption showing $(I\lambda^2)^{\delta}$ dependence with δ varying between $\sim$0.25 and 0.41, with some weak dependence on the charge state Z of the target material. This conclusion is further supported by fractional absorption measurements,[21] studies of the polarization and irradiance-angle dependence of the bremsstrahlung emission,[22,23] and of the energies and angular anisotropy of the fast-ion emission.[20,24,25] However, the high-energy continuum emission from plasmas produced by intense CO_2 lasers at comparable values of $I\lambda^2$ has not to date been so clearly characterized. Early experiments,[4,26] with nanosecond pulses indicated values of T_H similar to those obtained with 1-μm lasers for values of $I\lambda^2$ in the region of 10^{16} Wμm^2 cm^{-2}. The power dependence of the total x-ray intensity was also found to be similar to that obtained with shorter-wavelength irradiation,[27] although the absolute conversion efficiency was approximately 20 times less. However, in experiments at lower powers ($I\sim10^{12}$ W cm^{-2}) with long (40 ns) pulse CO_2 lasers, Stenz *et al.*[28] found $\delta\sim0.63$, corroborated with a similar dependence for the fast-ion blowoff, and in accordance with a steady-state flux-limited scaling law.[11,13]

In this paper we describe an investigation of the bremsstrahlung emission from plasmas produced by intense nanosecond CO_2 laser pulses in the intensity range 10^{13}–2×10^{14} W cm^{-2}. The emission has been characterized as a function of laser intensity and target material, and its dependence on laser beam polarization, prepulse condition, irradiation angle, and focus position have been determined. These results are compared with measurements of the fractional absorption,[29] electron-density distribution,[30] and high-harmonic emission levels from the plasma.[31–37]

II. EXPERIMENTAL CONDITIONS

Measurements of the x-ray continuum emission were made under a wide range of operating conditions with plane flat polished targets irradiated with the output of one arm of the COCO-II CO_2 laser system.

A. Characteristics of the laser pulse

The laser system provided energy in excess of 50 J in a single pulse of nominal nanosecond duration in a near-diffraction-limited beam, 80 mm in diameter.[32] The system uses uv preionized atmospheric-pressure discharges throughout with several saturable absorber gas-isolator cells in the am-

 0021-8979/79/063909-06$01.10

plifier chain. Because of saturation effects, the originally approximately Gaussian pulse emanating from the mode-locked oscillator and switchout stages is considerably modified during amplification. Initial investigations using a picosecond resolution linear-upconversion technique[33] indicate the pulse has a rise time typically of ~ 400 ps and a fall time of 800 ps to 1 nsec. An on-line prepulse monitoring scheme is capable of detecting levels of prepulse above 50 μJ and prelase above 50 kW and, in general, the pulse contrast ratio was $\sim 10^6$. The near-field energy distribution had peak intensity in a central peak ~ 20 mm in diameter surrounded by a high-intensity ring ~ 60 mm in diameter.[34] The beam was focused onto plane solid targets in a vacuum $\sim 5\times 10^{-5}$ Torr, by an $f/1.5$ 20 -cm focal length off-axis parabolic mirror. After accounting for various transmissions and reflection losses in transporting the beam to target, the maximum energy delivered on target in these experiments was ~ 45 J. The focal spot size had a measured half-energy diameter of $\sim 110\,\mu$m [35] and was limited by imperfections in the focusing mirror. Thus peak intensities of $\sim 2.4\times 10^{14}$ W cm^{-2} were deliverable on target with prepulse radiation levels of $< 2\times 10^{8}$ W cm^{-2}. Under these conditions, picosecond visible-light interferometry[30] established that no detectable plasma ($n_e < 10^{18}$ cm^{-3}) existed on the surface of the target prior to the incidence of the pulse.

Plane, flat-polished targets of Al, Be, C, and $(CH_2)_n$ were utilized in this study, each being aligned in the focal plane to an accuracy of $\sim 30\,\mu$m.

B. Conditions of the interaction

The extent of the x-ray emitting region of the plasma was determined by pinhole photography on Kodak SC-7 film. The camera had an aperture 15 μm in diameter and was situated 20 mm from the target. The film was shielded by a 25-μm Be filter, and a 1-kG magnetic field prevented film fogging effects due to superthermal electrons. A typical photograph is shown in Fig. 1. It can be seen that the emitting region is $\sim 150\,\mu$m in diameter and extends from the target surface by less than 100 μm. Spatially and temporally resolved electron-density measurements indicate the plasma-density profile has a steep density gradient, of scale length $\sim 10\,\mu$m, extending from $n_c \sim 2\times 10^{18}$ cm^{-3} through the

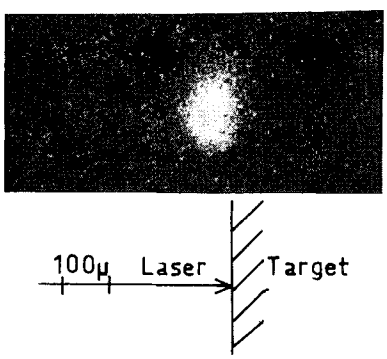

FIG. 1. X-ray pinhole photograph of an Al plasma. The incident intensity was $\sim 2\times 14$ W/cm^2.

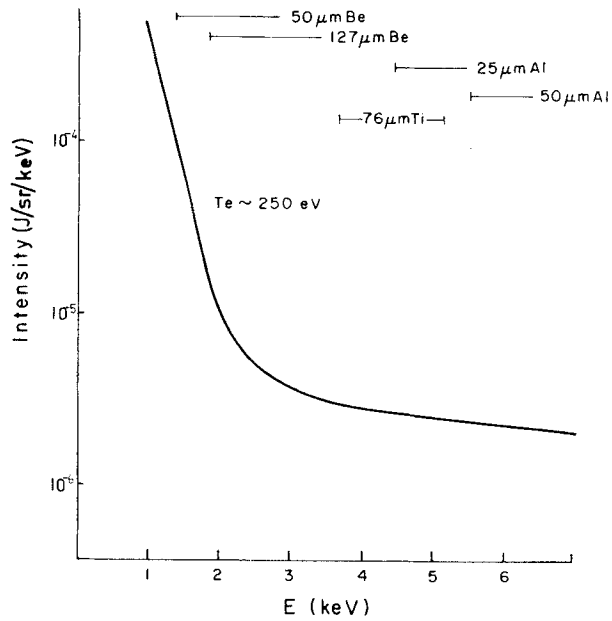

FIG. 2. The continuum spectrum obtained from a (CH_2) plasma. The ranges of the x-ray channels are shown.

critical density ($n_c = 10^{19}$ cm^{-3}) to a density approximately equal to that for equilibration between the radiation and plasma kinetic pressures ($\sim 7n_c$ for 2×10^{14} W cm^{-2}). This density wall moves away from the target surface with a velocity of $\sim 10^7$ cm s^{-1} during and immediately after the interaction. Since the fast-time-response x-ray detectors indicate the predominant x-ray emission occurs within 1–2 ns after the creation of the plasma, the x-ray photograph of Fig. 1 unambiguously establishes that the primary emitting region is restricted to a zone well behind the critical density.

A typical spectrum of the x-ray continuum in the low-energy range emitted by a plasma produced off a $(CH_2)_n$ target is shown in Fig. 2.[27] From the slope of the spectrum in the low-energy region, a value of the thermal temperature of $T_C \sim 250$ eV is deduced. This can be compared with values of T_C obtained from a study of the He-like and H-like resonance lines recorded with an x-ray crystal spectrograph from similar plasmas created off Al and Mg targets. From these investigations estimates of T_C of 300–400 eV at densities of $n_e > 10^{20}$ cm^{-3} were deduced. A superthermal temperature, T_H of 9.5 keV was inferred from the slope of the high-energy portion of the spectrum shown in Fig. 2.

The major difference between the x-ray emission spectrum obtained from plasmas produced by CO_2 lasers and those produced by Nd : glass lasers is the reduction in the observed intensity by more than an order of magnitude of the thermal component of the spectrum[27,36–39] from CO_2-laser-produced plasmas. As a consequence the superthermal component of the spectrum becomes dominant at a lower x-ray energy with 10-μm irradiation. In our investigations a significant fraction of the x-ray flux detected by even the lowest-energy x-ray detector channels was due to the superthermal portion of the spectrum. However, since the sensitivity of SC-7 film drops rapidly above a few keV, the pinhole photograph (Fig. 1) would not be as sensitive to the superthermal emission.

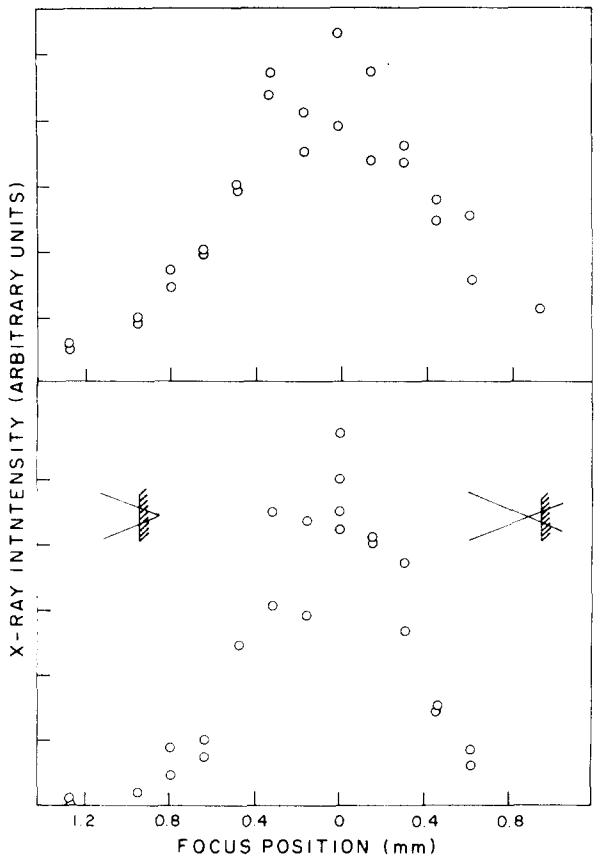

FIG. 3. The dependence of the x-ray intensity on focal position. The top curve corresponds to x rays between 5 and 25 keV and the bottom curve corresponds to x rays above 10 keV.

III. MEASUREMENTS OF SUPERTHERMAL X-RAY EMISSION

The superthermal x-ray emission from the plasma was examined under a wide range of operating conditions in the energy range 4 –30 keV with the aid of a number of detector-foil combinations. These utilized as active elements, surface barrier detectors (Ortec R-series), PIN detectors (Quantrad PIN 250), or photomultiplier scintillator combinations. In order to obtain reproducible spectra throughout this region care was taken to protect the detectors from both energetic electrons and x rays that originate outside the plasma region. The detectors were enclosed in a light-tight housing which had a foil entrance window. A collimator that consists of a 100-mm-long brass pipe with an inside diameter of ~ 10 mm ensured that only x rays originating in the plasma region were detected. An inside pipe thread was cut in the collimator to form a series of apertures in the beam path. A permanent magnet that provides a 1-kG field over a 1-cm region was placed in front of the collimator entrance to sweep away electrons from the detectors. Despite these precautions it was found that a significant fraction of the x rays of energy greater than ~ 25 keV recorded by the detectors originated outside the immediate plasma region. The most probable source of this signal is x-ray fluorescence of the aluminum target support structure caused by fast electrons emitted from the plasma.[38–40] Thus measurements of the plasma continuum beyond this energy range (~ 30 keV) were not reliable.

In the present experiments the values of T_H were determined using five surface-barrier detectors located in a cluster which was positioned ~ 40 cm from the target at angles of 60° with respect to the target normal and 80° to the axis of the laser irradiation. They were calibrated relative to each other in this configuration. This was achieved by using identical foils (both 50-μm Be and 25-μm Al were used) in front of each detector and comparing their respective signals for a number of laser shots. The typical shot-to-shot variation in signal was $\sim 7\%$ and the variations in sensitivity from detector to detector were less than 15% and did not depend on the foil used for the calibration.

In obtaining the values of T_H it has been assumed that the emission above 4 keV can be described by a single temperature. Because of the sensitivities of the detectors employed, these values of T_H are primarily determined from the spectral characteristics in the region from 5 to 24 keV. The error in T_H due to shot-to-shot variations in the detector signals is $\sim 10\%$ (for $T_H < 15$ keV). An iterative deconvolution procedure was used employing Henke's analytical expressions[41] for x-ray absorption coefficients in calculating foil transmissions and detector sensitivies.

A. Focal-spot dependence

The intensity of the hot x-ray component is very sensitive to the focusing conditions. Figure 3 shows the x-ray intensity detected by two of the detectors as the target is moved in and out of focus. The upper figure illustrates the transmission through 50-μm Al foil and detected by a surface-barrier detector, which corresponds to x rays of energy between 5 and 24 keV and the lower figure shows transmission through 75-μm Ti detected by a photomultiplier–NaI scintillator detector which is sensitive to x rays above 10 keV. The data were taken with Al targets with from 20 to 30 J of incident energy. The variation in incident energy is responsible for most of the observed scatter. It can be seen from Fig. 3 that the intensity of x rays of higher energy exhibits a stronger dependence on focus position than those of lower energy. Thus, the hot-electron temperature deduced from these distributions will also be dependent on focal position and has the form shown in Fig. 4. From Fig. 4 it is noted that this temperature has a peak value when the target is in a

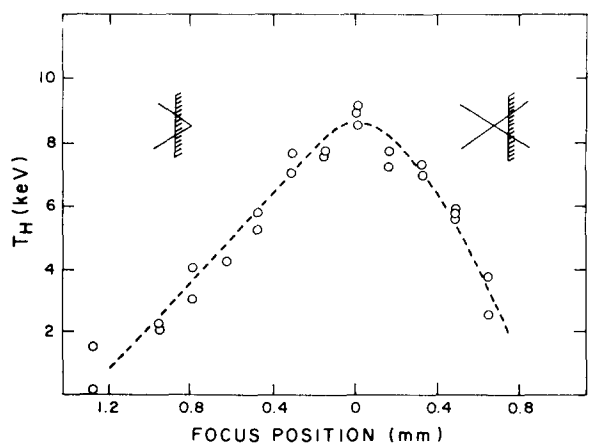

FIG. 4. The dependence of T_H on focal position.

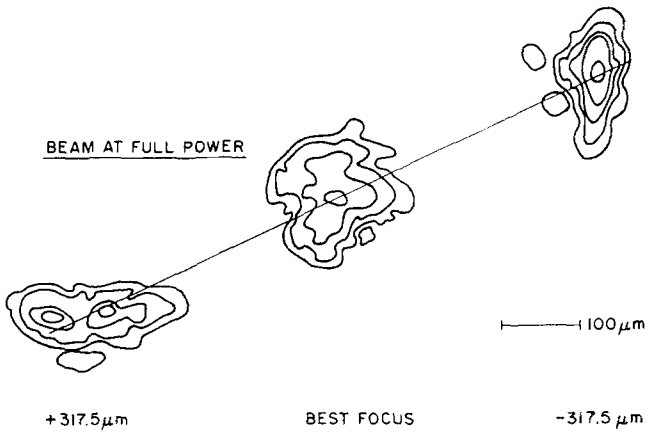

FIG. 5. The dependence of focal-spot intensity distribution on the distance from the best focus. Each successive intensity contour represents a change in intensity by a factor of 2.

position corresponding to best optical focus, and that the value of T_H drops by a factor of 2 in moving the beam focus by only 400 μm. Thus, in these experiments the maximization of high-energy x-ray flux and T_H could be utilized as a means of confirming optimum focus. Similarly, strong focal-spot dependence of the superthermal emission has been observed with Nd : glass lasers.[4,5,8] In these investigations comparable behavior appears to be evident in the x-ray emission at higher energies (above 40 keV).

During these investigations concurrent backscattered harmonic emission levels were also being recorded and a strong correlation was found between the intensity of scattered high-harmonic radiation[31,42] and the intensity of the superthermal x rays. However, measurements of the fractional absorption utilizing both infrared light balance and ion calorimetric techniques indicated no strong dependence of the absorption (typically ~40% for an irradiation angle of 20°) on focus position or target material.

Preliminary measurements of the focal-spot side on either side of focus had indicated that the variation in average intensity was not sufficient to explain the present results. More recently, the intensity distributions on either side of focus have been more carefully measured[35] and it is evident that it is difficult to rule out the variation in intensity distribution on target as the sole cause of the observed dependence of the x-ray emission on focal position. Figure 5 illustrates the change in focal-spot intensity distribution on either side of best focus. At best focus the focal spot is reasonably symmetric, but even 100 μm away from best focus the spot becomes elongated and begins to break up and exhibits localized hot spots. At positions further away from focus the beam breakup is more severe and it is not clear how to assign a value to the focal-spot size.

B. Dependence on irradiance angle

The dependence of the x-ray emission on irradiance angle is illustrated in Fig. 6. Although T_H changes only slightly as the irradiance angle is changed from 15° to 35° the intensity of x rays transmitted through 50-μm Al foil (5–25-keV x rays) is reduced by a factor of 3. The irradiance angle measurements were made with both *S*- and *P*- polarized incident laser light. Any dependence on polarization was less than the shot-to-shot scatter in the data.

Measurements made of the higher harmonics scattered off the plasmas under similar conditions indicate that their intensities exhibited a similar dependence on irradiance angle to that shown by the high-energy x-ray intensity. The ratio between successive harmonic intensities appeared to be relatively independent of irradiation angle or polarization. Concurrent measurements have revealed that the fractional energy absorbed drops from 45 to 30% from *P*-polarized light and from 30 to 25% for *S*-polarized light as the irradiance angle is varied from 15 to 40°. The observed dependence of the energetic x-ray intensity and the absorbed energy is consistent with the number of hot electrons being proportional to the absorbed energy.

Recently a study of the irradiance angle dependence of the superthermal x-ray emission from 1-μm laser-produced plasma has been reported.[20] The study has shown that T_H has an irradiance-angle dependence that is similar to previously reported energy-absorption measurements, while the superthermal x-ray flux exhibits a more enhanced irradiance-angle dependence. Because of the small *f* number of the focusing optics, the smaller values of kL (where k is the free-space wave vector of the incident radiation and L is density

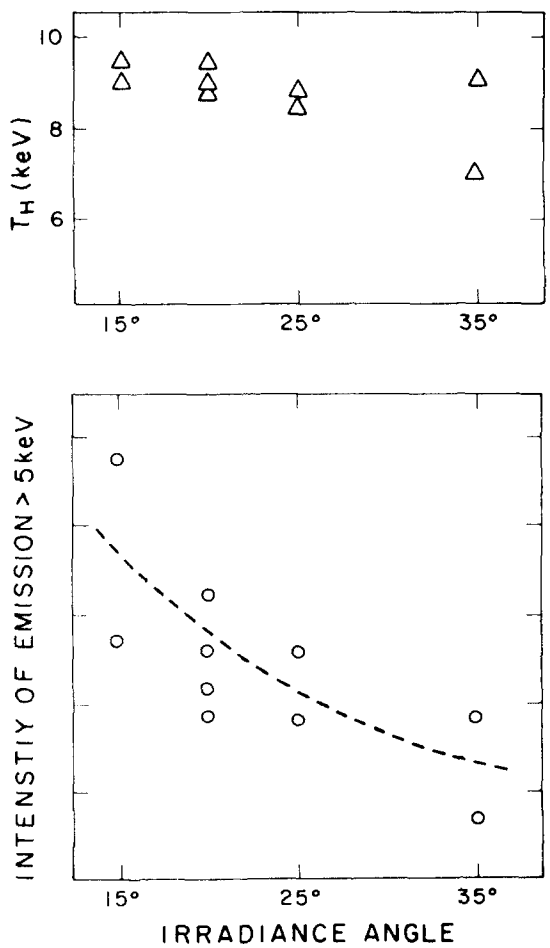

FIG. 6. The dependence of hot x-ray intensity (top curve) and T_H (bottom curve) on irradiance angle.

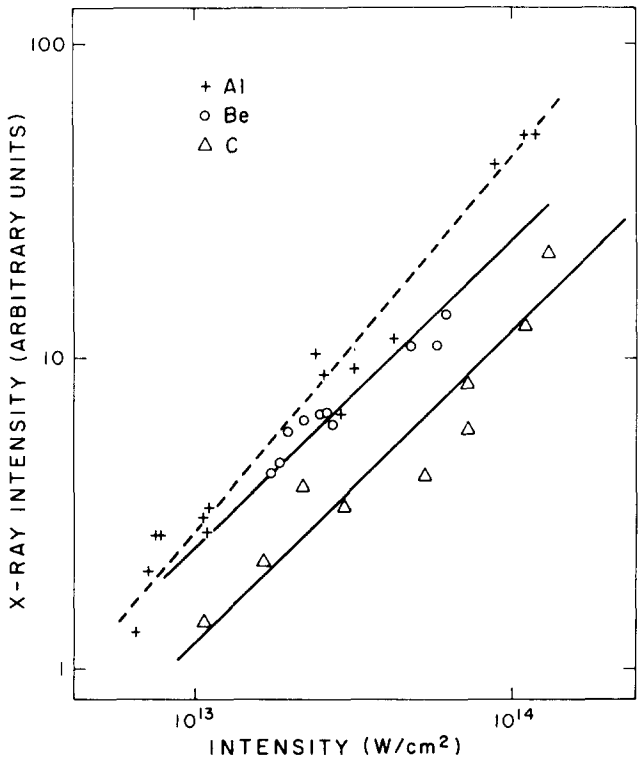

FIG. 7. The intensity dependence of the hot x-ray emission from various targets.

scale length), the larger radiation pressures, and the longer pulse lengths encountered in our experiments, we would not expect to observe a clear resonance peak in the absorption measurements as has been observed with glass-laser-produced plasmas.

C. Intensity dependence

The intensity dependence of the x-ray emission is illustrated in Fig. 7 for various targets. For Be and C the intensities have a power-law dependence of ~ 1, while for Al targets the power law appeared to be ~ 1.2. This difference may be due to the leakage of the intense Al line emission through the Al filters. The linear dependence of energetic x-ray intensity

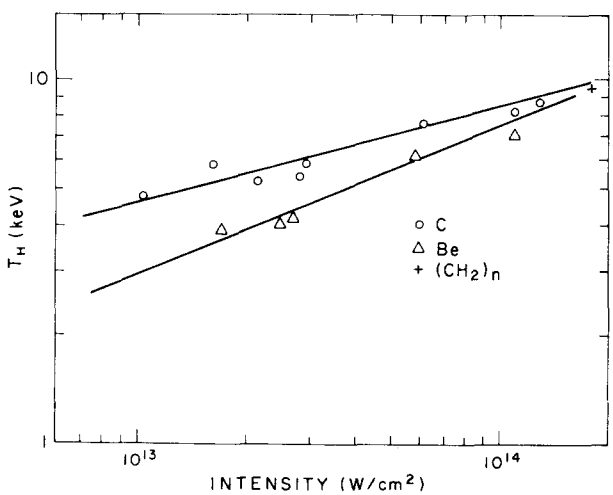

FIG. 8. The dependence of T_H on incident for Be and C targets.

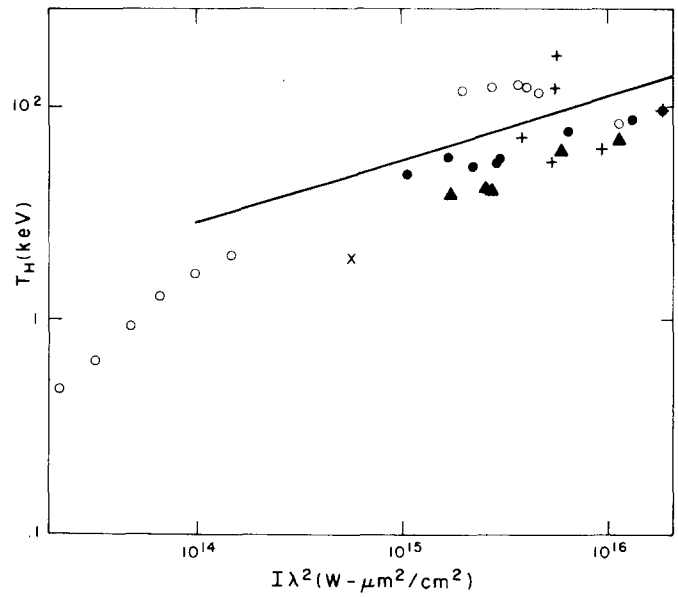

FIG. 9. Comparison of the present results (solid circles and triangles) with other CO_2-laser-produced plasmas; [LASL (Ref. 16) O for $I\lambda^2 > 10^{15}$, LLL (Ref. 38) +, INRS (Ref. 36) +, and Ecole Poly. (Ref. 28) O for $I\lambda_2 < 10^{14}$]. The solid line is representative of results with Nd : glass-laser-produced plasmas (Ref. 18).

on laser power, together with the observed independence of the fractional-energy absorption on laser intensity further substantiates the assertion that the number of hot electrons is proportional to the absorbed energy. A somewhat surprising result was the fact that the emission was more intense from Be targets than from C targets. The intensity had been expected to increase with increasing z.

The dependence of T_H on irradiance level is illustrated in Fig. 8. It is found to obey a power law of ~ 0.26 for C and ~ 0.39 for Be. Also included in Fig. 7 is a single measurement made from a polyethylene plasma. A similar weak dependence of T_H on target z and irradiation conditions has been noted recently with 1-μm irradiation.[18]

A scaling law of $T_H \sim (I\lambda^2)^{\sigma}$ is expected. These results clearly indicate that for $I\lambda^2 > 10^{15}$ σ is z dependent. We may compare our results to other CO_2-irradiation studies and investigations with 1-μm illumination as is shown in Fig. 9. Although absolute comparison between different experiments is not possible because of differences in focal-spot distributions, a general behavior of $T_H \sim (I\lambda^2)^{1/3}$ for $I\lambda^2 > 10^{14}$ does appear to be evident. This behavior is consistent with resonance absorption being the dominant absorption mechanism in this region.

IV. CONCLUSIONS

The superthermal x-ray emission from high-intensity CO_2-laser-produced plasmas exhibits characteristics similar to those obtained from glass-laser-produced plasmas when compared at equal values of $I\lambda^2$. The scaling of T_H with $(I\lambda^2)^{\sigma}$ has been confirmed for CO_2-laser-produced plasmas. Although the derived value of σ is somewhat target dependent, it is in agreement with values obtained from simulations which employ resonance absorption as the dominant laser-light-absorption mechanism.

ACKNOWLEDGMENTS

The authors would like to thank P. Burtyn and G.A. Berry for their able technical support.

[1]K. Büchl, K. Eidman, P. Mulser, H. Salzmann, and R. Sigel, Laser Interact. Relat. Plasma Phenom. **2**, 503 (1972).
[2]J.W. Shearer, S.W. Mead, J. Petruzzi, F. Rainer, J.E. Swain, and C.E. Violet, Phys. Rev. A **6**, 764 (1972).
[3]J.N. Olsen, G.W. Kuswa, and E.D. Jones, J. Appl. Phys. **44**, 2275 (1973).
[4]J.F. Kephart, R.P. Godwin, and G.H. McCall, Appl. Phys. Lett. **25**, 108 (1974).
[5]B.H. Ripin, P.G. Burkhalter, F.C. Young, J.M. McMahon, D.G. Colombant, S.E. Bodner, R.R. Whitlock, D.J. Nagel, D.J. Johnson, N.K. Winsor, C.M. Dozier, R.D. Bleach, J.A. Stamper, and E.A. McLean, Phys. Rev. Lett. **34**, 1313 (1975).
[6]F.C. Young, Phys. Rev. Lett. **33**, 747 (1974).
[7]V.W. Slivinsky, H.N. Kornblum, and H.D. Shay, J. Appl. Phys. **46**, 1973 (1975).
[8]K. Eidmann, M.H. Key, and R. Sigel, J. Appl. Phys. **47**, 2402 (1976).
[9]R.A. Haas, H.D. Shay, W.L. Kruer, M.J. Boyle, D.W. Phillion, F. Rainer, V.C. Rupert, and H.N. Kornblum, Phys. Rev. Lett. **39**, 1533 (1977).
[10]W.L. Kruer and J.M. Dawson, Phys. Fluids **15**, 406 (1972).
[11]R.L. Morse and C.W. Nielson, Phys. Fluids **16**, 909 (1973).
[12]J.J. Thompson, R.J. Faehl, W.L. Kruer, and S.E. Bodner, Phys. Fluids **17**, 973 (1974).
[13]H.H. Klein and W.M. Manheimer, Phys. Rev. Lett. **33**, 353 (1974).
[14]D.N. Forslund, J.M. Kindel, K. Lee, E.L. Lindeman, and R.L. Morse, Phys. Rev. A **11**, 679 (1975).
[15]K.G. Estabrook, E.J. Valeo, and W.L. Kruer, Phys. Fluids **18**, 1151 (1975).
[16]D.N. Forslund, J.M. Kindel, and K. Lee, Phys. Rev. Lett. **39**, 284 (1977).
[17]W.M. Manheimer, D.G. Colombant, and B.H. Ripin, Phys. Rev. Lett. **38**, 1135 (1977).
[18]K.R. Manes, H.G. Ahlstrom, R.A. Haas, and J.F. Holzrichter, J. Opt. Soc. Am. **67**, 717 (1977).
[19]F.C. Young and B.H. Ripin, Bull. Am. Phys. Soc. **22**, 1112 (1977).
[20]B. Luther-Davies, Opt. Commun. **23** 98 (1977).
[21]K.R. Manes, V.C. Rupert, J. M. Auerbach, P. Lee, and J.E. Swain, Phys. Rev. Lett. **39**, 281 (1977).
[22]J.E. Balmer and T.P. Donaldson, Phys. Rev. Lett. **39**, 1084 (1977).
[23]B. Luther-Davies, Appl. Phys. Lett. **32**, 209 (1978).
[24]J.S. Pearlman, J.J. Thompson, and C.E. Max, Phys. Rev. Lett. **38**, 1397 (1977).
[25]P. Wagli and T.P. Donaldson, Phys. Rev. Lett. **40**, 875 (1978).
[26]R.A. Haas, M.J. Boyle, K.R. Manes, and J.E. Swain, J. Appl. Phys. **47**, 1318 (1976).
[27]G.D. Enright, N.H. Burnett, and M.C. Richardson, Appl. Phys. Lett. **31**, 494 (1977).
[28]C. Stenz, C. Popovics, J. Virmont, A. Poquerusse, and C. Garban, J. Phys. (Paris) **38**, 761 (1977).
[29]D.M. Villeneuve, G.D. Enright, and M.C. Richardson, Bull. Am. Phys. Soc. **22**, 1059 (1977).
[30]R. Fedosejevs, I.V. Tomov, N.H. Burnett, G.D. Enright, and M.C. Richardson, Phys. Rev. Lett. **39**, 932 (1977).
[31]N.H. Burnett, H.A. Baldis, G.D. Enright, and M.C. Richardson, Appl. Phys. Lett. **31**, 172 (1977) and Bull. Am. Phys. Soc. **22**, 1077 (1977).
[32]M.C. Richardson, N.H. Burnett, H.A. Baldis, G.D. Enright, R. Fedosejevs, N.R. Isenor, and I.V. Tomov, Laser Interact. Rela. Plasma Phenom. **4A**, 161 (1977).
[33]P. Jaanimagi, M.C. Richardson, and N.R. Isenor, Opt. Lett. **4**, 45 (1979).
[34]N.H. Burnett, H.A. Baldis, G.D. Enright, M.C. Richardson, and P.B. Corkum, J. Appl. Phys. **48**, 3727 (1977).
[35]C. Joshi, G.D. Enright, and M.C. Richardson, NRC Report (unpublished).
[36]H. Pepin, B. Grek, F. Rheault, and D.J. Nagel, J. Appl. Phys. **48**, 3312 (1977).
[37]K.B. Mitchell and P.B. Lyons, Bull. Am. Phys. Soc. **20**, 1303 (1975).
[38]K.R. Manes (private communication) These results were obtained with paralene disk targets with the Valkyrie CO_2 laser. The results are qualified by limitations on measurement of the laser pulse duration and the focal spot intensity distribution.
[39]C.E. Violet and J. Petruzzi, J. Appl. Phys. **48**, 4984 (1978).
[40]D.V. Giovanelli, J.F. Kephart, and A.H. Williams, J. Appl. Phys. **47**, 2907 (1976).
[41]B.L. Henke and M.L. Schattenburg, Adv. X-ray Anal. **19**, 749 (1975).